University of Bristol - Explore Bristol Research
General rights

Scalable mode division multiplexed transmission over a 10-km ring-core fiber using high-order orbital angular momentum modes

GUOXUAN ZHU,[1] ZIYANG HU,[2] XIONG WU,[1] CHENG DU,[3] WENYONG LUO,[3] YUJIE CHEN,[1] XINLUN CAI,[1] JIE LIU,[1,*] JIANGBO ZHU,[2,4] AND SIYUAN YU[1,2]

[1]State Key Laboratory of Optoelectronic Materials and Technologies, School of Electronics and Information Engineering, Sun Yat-sen University, Guangzhou 510275, China
[2]Photonics Group, Merchant Venturers' School of Engineering, University of Bristol, Bristol BS8 1UB, UK
[3]Fiberhome Telecommunication Technologies Co. Ltd, Wuhan, 430074, China
[4]jiangbo.zhu@bristol.ac.uk
*liujie47@mail.sysu.edu.cn

Abstract: We propose and demonstrate a scalable mode division multiplexing scheme based on orbital angular momentum modes in ring core fibers. In this scheme, the high-order mode groups of a ring core fiber are sufficiently de-coupled by the large differential effective refractive index so that multiple-input multiple-output (MIMO) equalization is only used for crosstalk equalization within each mode group. We design and fabricate a graded-index ring core fiber that supports 5 mode groups with low inter-mode-group coupling, small intra-mode-group differential group delay, and small group velocity dispersion slope over the C-band for the high-order mode groups. We implement a two-dimensional wavelength- and mode-division multiplexed transmission experiment involving 10 wavelengths and 2 mode groups each with 4 OAM modes, transmitting 32 GBaud Nyquist QPSK signals over all 80 channels. An aggregate capacity of 5.12 Tb/s and an overall spectral efficiency of 9 bit/s/Hz over 10 km are realized, only using modular 4x4 MIMO processing with 15 taps to recover signals from the intra-mode-group mode coupling. Given the fixed number of modes in each mode group and the low inter-mode-group coupling in ring core fibres, our scheme strikes a balance in the trade-off between system capacity and digital signal processing complexity, and therefore has good potential for capacity upscaling at an expense of only modularly increasing the number of mode-groups with fixed-size (4x4) MIMO blocks.

References and links

1. G. Li, N. Bai, N. Zhao, and C. Xia, "Space-division multiplexing: the next frontier in optical communication," Adv. Opt. Photonics **6**(4), 413 (2014).
2. D. J. Richardson, J. M. Fini, and L. E. Nelson, "Space-division multiplexing in optical fibres," Nat. Photonics **7**(5), 354–362 (2013).
3. M. Koshiba, K. Saitoh, and Y. Kokubun, "Heterogeneous multi-core fibers: proposal and design principles," IEICE Electron. Express **6**(2), 98–103 (2009).
4. S. Randel, R. Ryf, A. Sierra, P. J. Winzer, A. H. Gnauck, C. A. Bolle, R. J. Essiambre, D. W. Peckham, A. McCurdy, and R. Lingle, Jr., "6×56-Gb/s mode-division multiplexed transmission over 33-km few-mode fiber enabled by 6×6 MIMO equalization," Opt. Express **19**(17), 16697–16707 (2011).
5. R. Ryf, H. Chen, N. K. Fontaine, A. M. Velazquez-Benitez, J. Antonio-Lopez, C. Jin, B. Huang, M. Bigot-Astruc, D. Molin, F. Achten, P. Sillard, and R. Amezcua-Correa, "10-Mode Mode-Multiplexed Transmission over 125km Single-Span Multimode Fiber," Proc. ECOC, PDP3.3 (2015).
6. B. Franz and H. Bülow, "Mode Group Division Multiplexing in Graded-Index Multimode Fibers," Bell Labs Tech. J. **18**(3), 153–172 (2013).

7. F. Feng, X. Guo, G. S. Gordon, X. Jin, F. Payne, Y. Jung, Q. Kang, S. Alam, P. Barua, J. Sahu, D. J. Richardson, I. H. White, and T. D. Wilkinson, "All-optical mode-group division multiplexing over a graded-index ring-core fiber with single radial mode," Proc. OFC, W3D.5 (2016).
8. M. Kasahara, K. Saitoh, T. Sakamoto, N. Hanzawa, T. Matsui, K. Tsujikawa, and F. Yamamoto, "Design of three-spatial-mode ring-core fiber," J. Lightwave Technol. **32**(7), 1337–1343 (2014).
9. N. Bozinovic, Y. Yue, Y. Ren, M. Tur, P. Kristensen, H. Huang, A. E. Willner, and S. Ramachandran, "Terabit-scale orbital angular momentum mode division multiplexing in fibers," Science **340**(6140), 1545–1548 (2013).
10. R. M. Nejad, K. Allahverdyan, P. Vaity, S. Amiralizadeh, C. Brunet, Y. Messaddeq, S. LaRochelle, and L. A. Rusch, "Orbital angular momentum mode division multiplexing over 1.4 km RCF fiber," Proc. CLEO, SW4F.3 (2016).
11. K. Ingerslev, P. Gregg, M. Galili, F. D. Ros, H. Hu, F. Bao, M. A. U. Castaneda, P. Kristensen, A. Rubano, L. Marrucci, S. Ramachandran, K. K. Rottwitt, Y. Morioka, and L. K. Oxenlowe, "12 Mode, MIMO-free OAM transmission," Proc. OFC, M2D.1 (2017).
12. D. Gloge and E. A. J. Marcatili, "Impulse Response of Fibers with Ring-Shaped Parabolic Index Distribution," Bell Labs Tech. J. **52**(7), 1161–1168 (1973).
13. C. Brunet, P. Vaity, Y. Messaddeq, S. LaRochelle, and L. A. Rusch, "Design, fabrication and validation of an OAM fiber supporting 36 states," Opt. Express **22**(21), 26117–26127 (2014).
14. P. Gregg, P. Kristensen, and S. Ramachandran, "13.4km OAM state propagation by recirculating fiber loop," Opt. Express **24**(17), 18938–18947 (2016).
15. C. Koebele, M. Salsi, L. Milord, R. Ryf, C. A. Bolle, P. Sillard, S. Bigo, and G. Charlet, "40km Transmission of Five Mode Division Multiplexed Data Streams at 100Gb/s with Low MIMO-DSP Complexity," Proc. ECOC, Th.13.C.3 (2011).
16. C. Simonneau, P. Genevaux, G. Le Cocq, Y. Quiquempois, L. Bigot, A. Boutin, M. Bigot-Astruc, P. Sillard, and G. Charlet, "5-mode Amplifier with Low Modal Crosstalk for Spatial Mode Multiplexing Transmission with Low Signal Processing Complexity," Proc. ECOC, We.2.4.2 (2015).
17. D. Soma, Y. Wakayama, K. Igarashi, T. Tsuritani, "Weakly-coupled FMF transmission for reduction of MIMO complexity," IEEE Summer Topical, TuE2.2 (2016).
18. D. Soma, Y. Wakayama, K. Igarashi, and T. Tsuritani, "Partial MIMO-based 10-Mode-Multiplexed Transmission over 81km Weakly-coupled Few-mode Fiber," Proc. OFC, M2D.4 (2017).
19. D. Soma, S. Beppu, Y. Wakayama, Y. Kawaguchi, K. Igarashi, and T. Tsuritani, "257-Tbit/s Partial MIMO-based 10-Mode C+L-band WDM Transmission over 48-km FMF," Proc. ECOC, M.2.E.3 (2017).
20. K. Shi, Y. Jung, Z. S. Eznaveh, J. C. A. Zacarias, J. E. Antonio-Lopez, H. Zhou, R. Zhang, S. Chen, H. Wang, Y. Yang, R. A. Correa, D. J. Richardson, and B. Thomsen, "10×10 MDM Transmission over 24 km of Ring-Core Fibre using Mode Selective Photonic Lanterns and Sparse Equalization," Proc. ECOC, M.2.E.2 (2017).
21. K. Balemarthy, A. Polley, and S. E. Ralph, "Electronic equalization of multikilometer 10-Gb/s multimode fiber links: Mode-coupling effects," J. Lightwave Technol. **24**(12), 4885–4894 (2006).
22. X. Jin, A. Gomez, K. Shi, B. C. Thomsen, F. Feng, G. S. D. Gordon, T. D. Wilkinson, Y. Jung, Q. Kang, P. Barua, J. Sahu, S. Alam, D. J. Richardson, D. C. O'Brien, and F. P. Payne, "Mode Coupling Effects in Ring-Core Fibers for Space-Division Multiplexing Systems," J. Lightwave Technol. **34**(14), 3365–3372 (2016).
23. D. Marcuse, "Microdeformation losses of single-mode fibers," Appl. Opt. **23**(7), 1082 (1984).
24. S. Ramachandran, P. Gregg, P. Kristensen, and S. E. Golowich, "On the scalability of ring fiber designs for OAM multiplexing," Opt. Express **23**(3), 3721–3730 (2015).
25. R. Murayama, N. Kuwaki, S. Matsuo, and M. Ohashi, "Relationship between mode coupling and fiber characteristics in few-mode fibers analyzed using impulse response measurement technique," J. Lightwave Technol. **35**(4), 650–657 (2017).
26. F. Feng, X. Jin, D. O'Brien, F. Payne, Y. Jung, Q. Kang, P. Barua, J. K. Sahu, S. U. Alam, D. J. Richardson, and T. D. Wilkinson, "All-optical mode-group multiplexed transmission over a graded-index ring-core fiber with single radial mode," Opt. Express **25**(12), 13773–13781 (2017).
27. L. B. Du and A. J. Lowery, "The validity of "Odd and Even" channels for testing all-optical OFDM and Nyquist WDM long-haul fiber systems," Opt. Express **20**(26), B445–B451 (2012).
28. J. L. Rebola and A. V. T. Cartaxo, "Q-factor estimation and impact of spontaneous-spontaneous beat noise on the performance of optically preamplified systems with arbitrary optical filtering," J. Lightwave Technol. **21**(1), 87–95 (2003).
29. G. Labroille, B. Denolle, P. Jian, P. Genevaux, N. Treps, and J. F. Morizur, "Efficient and mode selective spatial mode multiplexer based on multi-plane light conversion," Opt. Express **22**(13), 15599–15607 (2014).

1. Introduction

Recently, multiplexing techniques utilizing the spatial or mode domain of light over multi-core fibers (MCFs) or multi-mode fibers (MMFs) have been intensively investigated aiming at breaking the nonlinear Shannon limit of the single mode fiber (SMF) capacity [1, 2]. Compared with the schemes implemented over MCFs where multiple single-mode cores must be sufficiently spaced to suppress crosstalk (XT) [3], techniques based on MMFs can increase

the number of transmission channels within a limited aperture and thus increase the capacity density of optical fibers [4].

Conventional approaches based on MMFs are divided into two categories: the multi-input multi-output (MIMO) digital signal processing (DSP) based approaches and the MIMO-free approaches. MIMO-based approaches include both space division multiplexing (SDM) and mode division multiplexing (MDM) implemented using few-mode fibers (FMFs) or MMFs [4, 5]. The main concern over their scalability is the complexity of MIMO DSP which increases with the square of the number of channels and with the differential group delay (DGD) among channels. For instance, in a 10-mode-multiplexed FMF transmission system, 20x20 MIMO signal processing at the receiver was required to compensate the mode coupling [5]. The ever-growing DSP complexity would be impractical in real-time implementations due to high hardware cost and power consumption, and would force frequent hardware upgrades to systems as channel count increases.

MIMO-free approaches mainly include mode-group multiplexing [6, 7] and orbital angular momentum (OAM) mode multiplexing [8–11]. They aim to suppress crosstalk among all channels with large differential effective refractive indices (Δn_{eff}) between modes or mode groups (MGs). MG multiplexing [6, 7] in graded index fibers (GIFs) typically employs all modes in each near-degenerate MG as one channel, therefore the capacity resource is under-utilized. In addition, the intra-MG DGD would also cause performance degradation. OAM multiplexed communications are typically implemented over ring core fibers (RCFs). RCFs supporting single-radial-order modes were initially proposed in the 1970s [12]. The principal strategy in OAM RCF design is to increase Δn_{eff} between OAM modes in the same MG to achieve MIMO-free transmission, typically using high contrast (such as air core [13]) fibers. To suppress modal XT over km-scale propagation, $\Delta n_{eff} > 1\text{x}10^{-4}$ is typically required [9], and this requirement should become more critical when the distance is further increased. The most successful demonstrations of OAM-MDM based MIMO-free data transmission so far are realized over the distances of 1-2 km [9–11]. Recently, an air core fiber that supports good quality OAM mode transmission has been demonstrated, in which the intra-MG Δn_{eff} of up to $1.7\text{x}10^{-4}$ is achieved [14]. However, the coupling between spin-orbit aligned and anti-aligned modes in the same MG generally > -10 dB after 13.4 km transmission. To further increase the separation and consequently the MIMO-free transmission distance would be technically challenging.

Meanwhile, weakly-coupled FMF transmission incorporating partial MIMO processing has recently been proposed to decrease the DSP complexity, in which FMFs with large Δn_{eff} between MGs (for graded-index FMFs) or non-degenerate modes (for step-index FMFs) are employed to ensure low inter-MG/mode coupling, so that only smaller MIMO blocks are required to equalize the XT between intra-MG/degenerate modes [15–19]. However, the DSP simplicity of such schemes is not sustainable in FMFs supporting high-order MGs, as the number of near-degenerate modes in each group of the graded-index FMFs and DGD between degenerate modes (e.g. LP31a/b, etc.) in the step-index FMFs increases with the mode order.

On the other hand, although MIMO-free transmission in RCFs over long distance is challenging, RCFs still have significant potential of increasing the capacity-distance product with low DSP complexity in fiber MDM systems [20]. In single-radial-mode RCFs, the number of degenerate modes in each high-order MG (and therefore the MIMO block size) is fixed at 4, reducing the DSP complexity significantly for high order modes. Furthermore, compared with the conventional MMFs that exhibit strong mode coupling among high order MGs [21], in RCF the coupling coefficient between adjacent MGs significantly decreases with the increasing azimuthal mode order due to increasing Δn_{eff} [22].

Therefore, in this paper, we propose a scalable fiber MDM scheme (as shown in Fig. 1) by utilizing high-order OAM modes in graded-index (GI) RCFs, in which MGs are de-coupled by the large inter-MG Δn_{eff} and only 4x4 MIMO equalization is needed to deal with intra-MG

mode coupling. In addition, low DGD among modes within each high-order MG is ensured by reducing the intra-MG Δn_{eff}, and thus to further decrease the complexity of 4x4 MIMO equalization. The proposed scheme shows good potential for up-scaling fiber MDM system performance (e.g., in terms of capacity-distance product) without disproportionally increasing the MIMO processing complexity. For proof-of-principle demonstration, we design and fabricate a GIRCF optimized for high capacity transmission with minimized MIMO requirements, and demonstrate an OAM-MDM transmission experiment over a 10-km GIRCF, in which successful transmission of 8 OAM modes belonging to 2 adjacent high-order MGs, each carrying 10 wavelengths of 32-GBaud QPSK signal, is achieved with the measured BER below the 20% soft-decision forward error correction (FEC) limit of 2.4 × 10^{-2}. Signals are recovered with a low memory-length (15 taps) 4x4 MIMO equalizer for each MG.
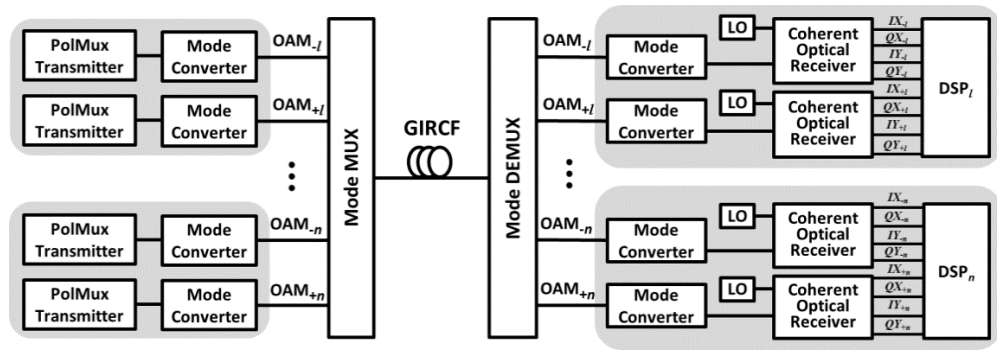

Fig. 1. Block diagram of the proposed scalable MDM scheme utilizing high order OAM modes in GIRCF. LO: local oscillator; DSP_i: digital signal processing module for the ith OAM mode group including OAM modes $< \pm i, \pm s >$ ($i = l, \dots n$, in which $l > 1$; $\pm i$ being the azimuthal mode order and $\pm s$ being the left- or right-hand circular polarizations).

2. Design, fabrication, and characterization of the GIRCF

In the GIRCF design, we aim to: (1) provide large inter-MG Δn_{eff} thereby de-coupling MGs, (2) soften the radial index gradient thereby making the fiber less susceptible to perturbations such as micro-bending [23], (3) reduce intra-MG Δn_{eff} thereby reducing the DGD among intra-MG modes, and (4) eliminate the spin-orbit-coupling-induced mode purity impairment [24] by removing the step refractive index (RI) interface. The generic index profile of GIRCFs we propose can be expressed as

$$n(r) = n_{\max} \sqrt{1 - \delta \left[\frac{2(R-r)}{W} \right]^{\alpha}} \tag{1}$$

$$\delta = \frac{n_{\max}^2 - n_{\min}^2}{n_{\max}^2} \tag{2}$$

where R is the radius of the RI ring profile crest, W is the ring core width (see Fig. 2(a)), α is the profile exponent, $n_{\max}$ and $n_{\min}$ are the maximum and minimum material refractive indices, respectively. δ describes the index contrast between core and cladding.

Given the maximum core-cladding index contrast ($n_{\max} - n_{\min} \approx 0.025$) afforded by our fiber fabrication technique, the number and index separation of MGs in GIRCF are primarily subject to the parameters R and W. Figure 2(a) shows the index profile of the GIRCF demonstrated in this paper, where $\Delta n = n - n_{cladding}$, and OAM mode-groups up to $|l| = 5$ at $\lambda = 1550$ nm are supported. $R = 7.6$ μm is selected to produce three MGs of $\Delta n_{eff} > 2 \times 10^{-3}$, while $W = 3.8$ μm to ensure the single-radial-mode condition.

The calculated effective RI n_{eff} of all guided MGs are shown in Fig. 2(b). In RCFs, the inter-MG Δn_{eff} increases with mode order, making higher order MGs more suitable for low crosstalk transmission. Also note that the $|l| = 1$ MG consists of the HE_{21}, TE_{01} and TM_{01} modes that are not degenerate ($\Delta n_{eff} \sim 10^{-4}$) and the intra-MG DGD after a 10-km propagation is considerable (~ 1 ns). Consequently, the $|l| = 1$ OAM MG is not suitable for low memory-length intra-MG MIMO processing. It is therefore permissible to allow smaller inter-MG Δn_{eff} between lower order MGs as they are not used for transmission. Generally, for this GIRCF, the inter-MG Δn_{eff} for $|l| \geq 3$ is $> 2 \times 10^{-3}$ for sufficient suppression of inter-MG coupling. The intra-MG Δn_{eff} is minimized to $\sim 1 \times 10^{-5}$ with $\alpha = 2$, leading to strong coupling but low DGD among modes within each MG. The group velocity dispersion (GVD) characteristics has also been calculated and plotted in Fig. 2(d), with all modes exhibiting very small GVD slope conducive to wavelength-division multiplexing (WDM) transmission.

The GIRCF is fabricated using a conventional plasma enhanced chemical vapor deposition (PECVD) process. The fabrication error of the fiber cladding diameter is $< \pm 0.5$ μm, and the ellipticity is less than 3%. A small low RI trench is introduced by Fluorine (F) doping around the ring core to enlarge the index contrast. Figure 2(c) shows an optical microscope image of the fiber cross section and the measured RI profile. The fiber is wound on a standard 18 cm diameter spool.
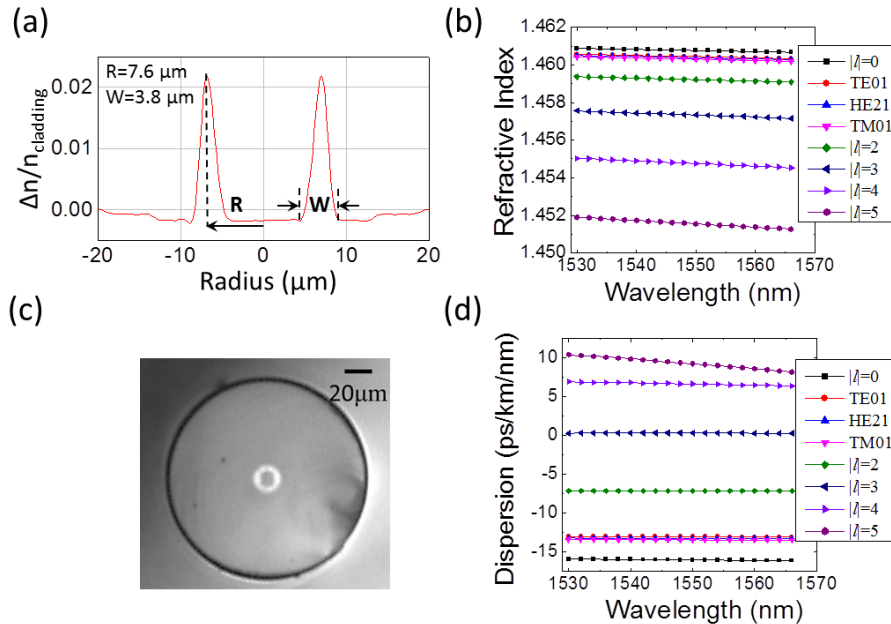

Fig. 2. (a) Measured RI distribution and (c) cross-sectional diagram of the fabricated GIRCF; calculated (b) effective refractive indices and (d) GVD characteristics of the guided mode groups as a function of wavelength.

By exciting and detecting OAM eigen-modes individually over a 10-km GIRCF, the measured attenuation is ~ 1 dB/km in average for all groups, and the mode dependent loss (MDL) for all modes among MGs $|l| \geq 3$ is less than 0.5 dB over 10 km. The relatively high fiber attenuation, which is the limiting factor to the transmission distance in the following transmission experiment, is due to unexpected fluctuations in the F-doping process during fiber preform fabrication. By further optimizing the fabrication process, a much lower attenuation is attainable in such RCFs (e.g., 0.2 ~0.3 dB/km [25,26]). On the other hand, the calculated and measured DGD values at the wavelength of 1550 nm agree very well as shown in Fig. 3. The increasing DGD between MGs reflects the increasing inter-MG Δn_{eff}, while the

intra-MG DGD is almost constant for all MGs either from calculations or measurements, indicating a low memory-size requirement on MIMO DSP.
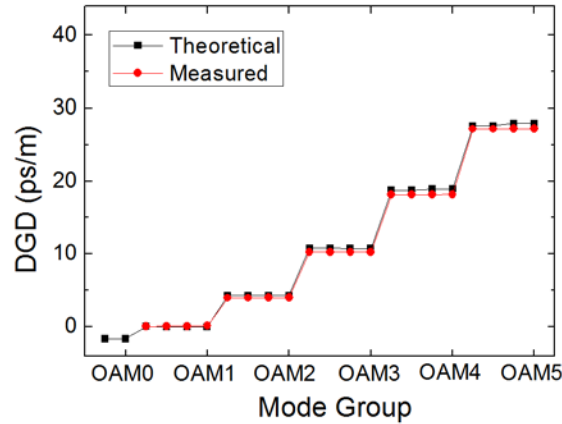

Fig. 3. Calculated and measured DGD of all mode groups in GIRCF at 1550 nm.

Table 1. The in-fiber effects induced crosstalk of high-order OAM MGs ($|l|$ = 3, 4 and 5) over 9.8-km GIRCF.

Crosstalk (dB)		Output MG		
		$|l|$ = 3	$|l|$ = 4	$|l|$ = 5
Input MG	$|l|$ = 3	0	−11.04	−14.96
	$|l|$ = 4	−9.58	0	−13.60
	$|l|$ = 5	−14.35	−13.01	0

The XT values among high-order MGs ($|l| \geq 3$) are characterized respectively with two GIRCF samples (200-meter and 10-km) and with the rest of optical setup (excluding GIRCF) in measurements unchanged. By comparing their results and eliminating the XT induced in OAM mode excitation and detection, an effective inter-MG XT matrix over ~9.8-km is then obtained, as shown in Table 1, more explicitly characterizing the MG coupling in GIRCF induced solely by in-fiber effects (including fiber imperfection, bending, etc.). The inter-MG coupling between MGs $|l|$ = 4 & 5 is ~-13.3 dB in average, which is lower than that between MGs $|l|$ = 3 & 4 (~-10.25 dB), in accordance with the increasing inter-MG Δn_{eff} with MG order. It can be deduced accordingly that the coupling coefficient (h) caused by in-fiber effects is in average 4.7×10^{-3} km^{-1} between $|l|$ = 4 & 5 and 9.4×10^{-3} km^{-1} between $|l|$ = 3 & 4. To implement OAM-MDM transmission with GIRCF over greater distances than 10 km, meanwhile avoiding DSP for inter-MG signal recovery, much lower in-fiber coupling coefficients are essential. Such a requirement coincides with the incentive mentioned above to lower the fiber attenuation, as currently the in-fiber coupling in GIRCF is predominantly contributed by the undesired discrepancy in F-doping during fabrication. Low coupling coefficients (e.g., $< 1 \times 10^{-4}$ km^{-1}) can be reasonably expected in future GIRCFs with improved fabrication [24]. The light source used for the XT measurement is the amplified spontaneous emission (ASE) output from a C-band Erbium-doped fiber amplifier (EDFA), and the overall low inter-MG XT achieved with this wide-band source shows the potential of GIRCF in carrying the two-dimensional multiplexed (i.e., OAM-MDM and WDM) signals. For the 10-km transmission experiment below, the two groups of $|l|$ = 4 and 5 will be employed for their lower XT.

3. Demonstration of proposed OAM-MDM scheme

With the GIRCF supporting low inter-MG XT and low intra-MG DGD for high-order MGs, the proposed OAM-MDM scheme shows more realistic DSP scalability: only a fixed-size (4x4) modular MIMO equalizer with relatively low memory length is needed for the signal recovery of each MG, and inter-MG coupling is suppressed due to the optical isolation of large inter-MG Δn_{eff}. As a proof-of-principle demonstration, we show here an 8-mode OAM-MDM (using OAM modes in MGs $|l|$ = 4 and 5) and 10-λ WDM data transmission system over the 10-km GIRCF, and the system implementation is shown in Fig. 4. 10 optical carriers from external cavity lasers with wavelengths ranging from 1547.71 nm to 1551.31 nm with a 0.4-nm/50-GHz channel spacing are combined by a wavelength multiplexer. Then the 10 WDM signals are obtained by modulating the carriers with 32-GBaud Nyquist-QPSK signals from an arbitrary waveform generator (AWG) with an I/Q modulator. The Nyquist filter is a square root raised cosine electrical filter with a 3-dB bandwidth of 0.6X symbol rate and a roll-off factor of 0.1. The sample rate of the digital-to-analog converter (DAC) is 64 GSa/s and the modulated electrical data sequence is pseudo-random binary sequence (PRBS) with pattern length of 2^{18} −1. Here note that due to the device limitation, all the WDM channels are modulated by one electrical signal. Insufficient decorrelation between WDM channels will overestimates the performance of the practical WDM systems with individual optical carriers carrying different data patterns, considering the inter-WDM-channel XT. However, this performance overestimation can be significantly mitigated by keeping sufficient guard band intervals between adjacent WDM channels (normally no less than 20% optical signal bandwidth/wavelength channel) [27]. In our experiment, the WDM guard gap is more than 25% optical signal bandwidth/wavelength channel, as shown in Fig. 7(c). In addition, highly correlated bit patterns of optical waveforms in neighboring optical channels will also cause non-linear signal degradation of WDM optical signals [27], which can be neglected in relatively short-distance transmission system (~10km fiber length in our experiment).
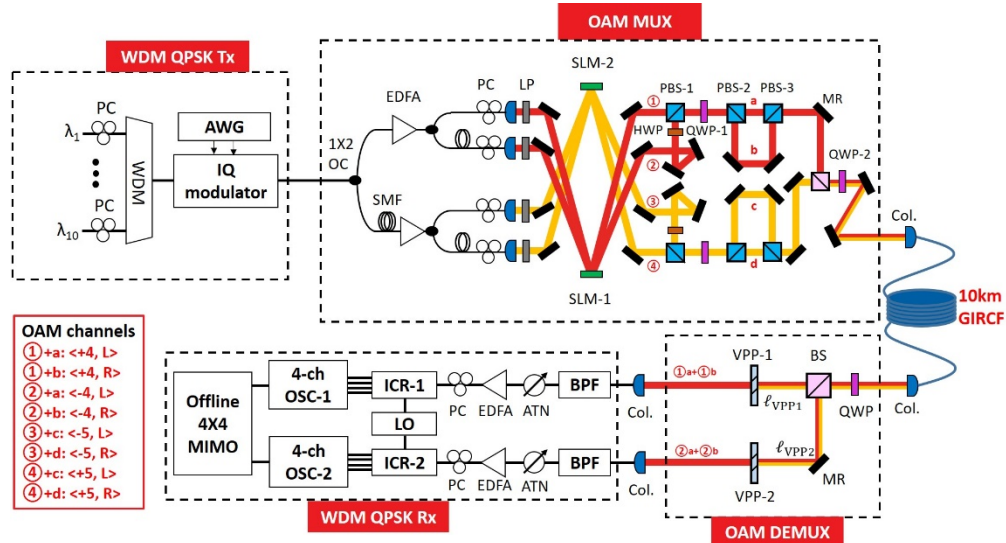

Fig. 4. Experiment setup. ECL: external cavity laser; WDM: wavelength division multiplexer; EDFA: erbium-doped fiber amplifier; PC: polarization controller; OC: optical coupler; SMF: single-mode fiber; LP: linear polarizer; SLM: spatial light modulator; PBS: polarizing beam splitter; HWP: half-wave plate; MR: mirror; QWP: quarter-wave plate; Col.: collimator; BS: beam splitter; VPP: vortex phase plate; ATN: attenuator; ASE: amplified spontaneous emission noise; OC: optical coupler; OTF: optical tunable filter; ICR: integrated coherent receiver.

The WDM signals are split by a 1x2 optical coupler (OC) and amplified by two Erbium-doped fiber amplifiers (EDFAs) (one of them delayed with a 10-meter SMF patch cord for decorrelation) to feed the mode MUX sections of the two OAM groups (i.e., $|l| = 4$ and 5). Each branch of light is then evenly split and decorrelated again (each with a 2-meter SMF). After collimation and linearly polarization, the two Gaussian beams from each branch are reflected by a phase-only spatial light modulator (i.e., SLM-1 and SLM-2 in Fig. 4) for conversion to OAM modes $l = + 4$ and $+ 5$, respectively. The OAM modes off each SLM, for example the pair ① and ② reflected by SLM-1, are combined using a polarizing beam splitter (i.e., PBS-1) as orthogonally polarized channels, after one of them passing a half-wave plate (HWP) for a 90-degree rotation of polarization. The two modes in each pair also exhibit opposite OAM orders (i.e., $l = \pm 4$) as they experience an odd difference in the number of reflections from SLM-1 to PBS-1, and then are converted to opposite circular polarizations (CPs) with a quarter-wave plate (i.e., QWP-1). These two CP OAM modes are again split into a group of four linearly polarized channels (i.e., $l = \pm 4$ and horizontally/vertically polarized) using PBS-2. Two of the channels in each group are decorrelated over ~80 cm after mirror reflections (i.e., along path **b**) and combined with the other two (in path **a**) using PBS-3. QWP-2 is used for imparting left- and right-CPs to the four channels in each group, so that the four decorrelated channels encompass the four modes (i.e., $\pm l$ and left-/right-CP) in each group of $|l| = 4$ or 5. The OAM and polarization states of all eight channels, each represented by its specific path through the OAM MUX section (e.g., ① + a), are shown in the red box in Fig. 4. The eight OAM modes are multiplexed and coupled into the 10-km GIRCF. The total insertion loss of this bulk-optics mode multiplexer is ~8 dB including the coupling loss into the fiber, while the loss of the fiber transmission is ~10 dB.

After fiber transmission, all output modes from the fiber are converted into linear polarizations and split into two branches. These two branches of light are imparted with two opposite vortex charges ($\pm m$) with two commercial vortex phase plates (VPPs) respectively, and the two orthogonally polarized OAM modes of $l = \mp m$ in each branch are converted into Gaussian beams, feeding two SMF-pigtailed dual-polarization integrated coherent optical receivers (ICRs). MGs of $|l| \neq m$ are spatially filtered out by the SMFs.

At the receiver, the optical signals are combined with the ASE noise before being amplified and filtered by a 50-GHz optical filter to improve the receiver sensitivity [28]. After detection by the two ICRs, the 8 output electrical waveforms (including the I/Q for each mode) are recorded by an 8-channel real-time oscilloscope (Teledyne LeCroy 10-36ZI) operated at 80-GSa/s and processed offline by 4x4 MIMO equalizers operated in blind mode with their coefficients of 16 FIR filters updated using the constant modulus algorithm (CMA).
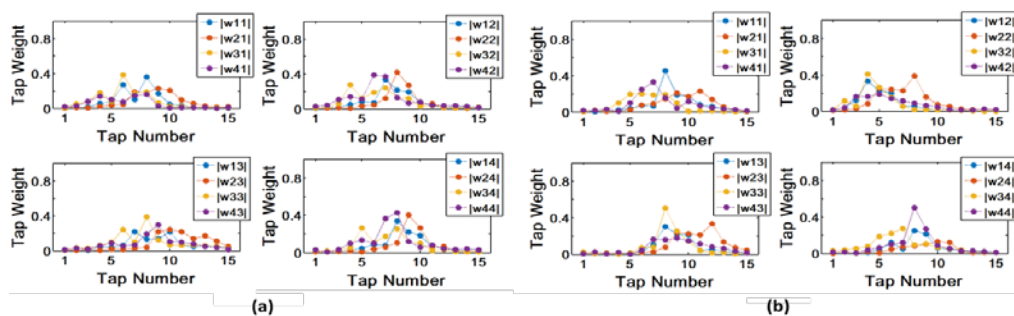

Fig. 5. The absolute values of complex tap weights of the four FIR filters to equalize the four modes in mode group (a) $|l| = 4$ and (b) $|l| = 5$.

Figure 5 shows the convergent tap weights of the 16 FIR filters after 30 iterations of updating using the CMA algorithm for both MGs of $|l| = 4$ and 5. The number of taps in each filter is set to 15, which is sufficient to cover the DGD in each group. In Fig. 6(a), the

measured bit-error-rate (BER) curves as a function of optical signal-to-noise ratio (OSNR) for all OAM modes at 1549.71 nm are plotted. BER measurements for two cases, including with OAM XT only (one wavelength and all 8 modes) in the back to back (B2B) configuration, and with all XT (with all 10 wavelengths and all 8 modes) after 10-km GIRCF transmission, are performed to identify the penalty sources. The B2B configuration has been implemented with a short length of GIRCF (~10 m) between the OAM MUX and DEMUX, and the BER evaluation for the two polarization signals of each OAM mode is performed together. As a result, two BER curves are presented for each OAM MG measurement in Fig. 6(a).
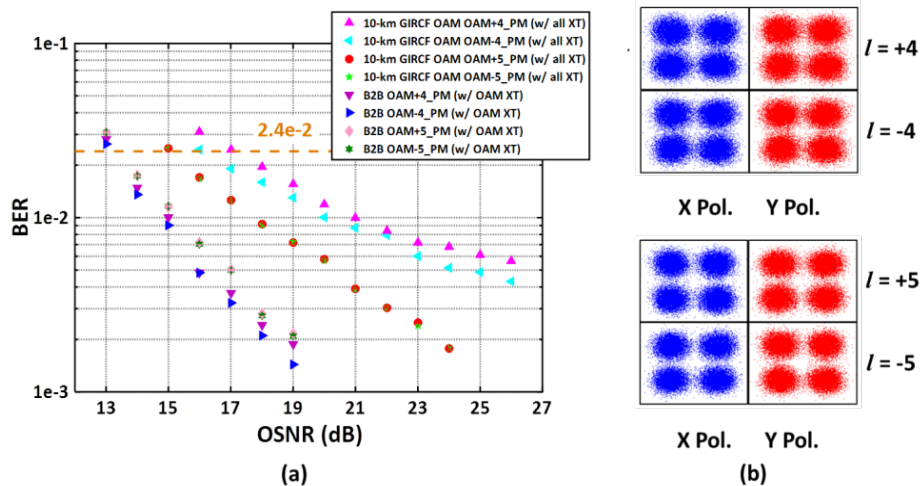
Fig. 6. (a) BER vs. OSNR at wavelength of 1549.71 nm after 10-km GIRCF transmission, and (b) constellations of the received signals with the best measured BERs at wavelength of 1549.71 nm after 10-km GIRCF transmission.

As shown in Fig. 6(a), compared with the B2B case with OAM XT, the average OSNR penalty for the 32-GBaud Nyquist QPSK signals with all XT after 10-km GIRCF transmission is less than 3 dB (around 2 dB and 3.5 dB for $|l| = 5$ and $|l| = 4$ group, respectively) at the BER of 2.4×10^{-2} (20% soft-decision FEC threshold). Compared with the BER performance of the mode group $|l| = 5$, there is an error floor at BER of ~5×10^{-3} for that of the mode group $|l| = 4$ with all XT after 10-km GIRCF transmission, which might be resulted from the relatively larger crosstalk from neighboring mode groups for the mode group $|l| = 4$ (see Table. 1). Constellations of the recovered 32-Gbaud Nyquist QPSK signals after 10-km GIRCF transmission at their best OSNRs are shown in Fig. 6(b). Figure 7(a) illustrates the measured BERs of all 8 modes over the 10 WDM channels, and those of all 80 channels are below the FEC threshold, achieving successful transmission of the OAM-MDM-WDM signals.
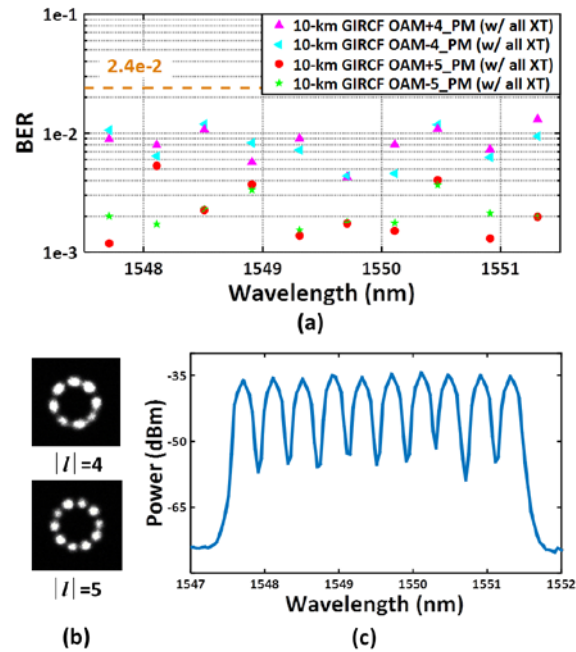
Fig. 7. (a) Measured BERs of all 80 channels after 10-km GIRCF transmission; (b) Observed intensity profiles of multiplexed modes from groups $|l|$ = 4, 5 after 10-km GIRCF transmission; (c) Optical spectra of all the 10 wavelength channels.

4. Conclusion and discussion

In this paper, we have proposed a scalable MDM scheme by utilizing high-order OAM modes in RCFs. Only 4x4 MIMO equalization is required to deal with intra-MG mode coupling in this scheme and crosstalk between weakly-coupled high-order MGs of the RCF can be neglected due to the large inter-group effective index differences. The proposed OAM-MDM scheme can be potentially up-scaled by modularly increasing the number of high-order mode groups and fixed-size 4x4 MIMO blocks without increasing the MIMO processing complexity, which affords a good balance between system capacity and complexity. We have also experimentally demonstrated this scheme by designing and fabricating a GIRCF, which is optimized for the two-dimensional WDM-MDM multiplexing scheme, and implement an 8-mode MDM transmission over 10-km GIRCF with 10 WDM wavelengths on each mode. At each wavelength, the 8 OAM mode channels – belonging to two adjacent MGs – are de-multiplexed in groups of 4, and recovered by two 4x4 modular MIMO equalizers. A total capacity of 5.12 Tb/s is achieved by loading each of the 80 channels with 32GBaud Nyquist QPSK signals, with in-band SE of 16 bit/s/Hz per WDM channel and overall SE of 9 bit/s/Hz across the WDM band.

The proposed RCF-based MDM scheme in this paper holds promising potential for applications such as metro-scale inter-data-center networks, which typically spans 80 ~120 km and require to significantly increase the single-wavelength capacity with low-complexity DSP module. In the present experiment with GIRCF, multiplexing more than two MGs for higher system capacity is hindered mainly by the insertion loss of more complicated MUX optics, which can be addressed in future study incorporating more compact and lower loss MUX/DEMUX solutions (e.g., < 2 dB [29]). The transmission distance is limited by the power budget due to high losses in fiber transmission. Future study will mainly focus on the improvement of fiber fabrication process to produce fibers of much lower loss (< 0.3 dB/km) and inter-MG coupling (< 1×10^{-4} km^{-1}), to enable the increase in both MG number and

transmission distances, so that the capacity-distance product can be up-scaled while maintaining the low MIMO complexity.

Funding

Acknowledgments